

Experimental Investigations of Ion–Molecule Reactions Relevant to Interstellar Chemistry

Dieter Gerlich

Fakultät für Physik, Universität Freiburg, D 7800 Freiburg, Germany

Based on the method to confine charged particles in inhomogeneous radiofrequency fields, two experimental set-ups have been developed for the study of ion–molecule reactions approximating interstellar conditions. The central part of the first apparatus is a variable-temperature ion trap (10–300 K), ring-electrode or 22-pole geometry). Long trapping and interaction times lead to high sensitivity, and allow one to determine very small rate coefficients, *e.g.* for radiative association. In the second apparatus a slow guided ion beam is superimposed coaxially with a supersonic neutral beam, combining the advantages of internally and translationally cold neutrals (also for condensable gases) with the kinematic compression resulting from the merged beam geometry. This technique enables one to determine absolute integral cross-sections over a wide range of collision energies, especially at energies of astrophysical interest. The internal temperature of the primary ions can be varied between 15 and 300 K. Both machines have been used to study a variety of ion–molecule reactions of interstellar interest. In this contribution new results are presented for the fine structure, rotational and isotope effects on the reaction $N^+ + H_2 \rightarrow NH^+ + H$. Rate coefficients have been determined at temperatures between 15 and 300 K using the ion trap, while state-specific cross-sections have been measured in the beam apparatus at collision energies between 1 and 500 meV. The experiments corroborate earlier conclusions that 17 meV are required for NH^+ formation from $N^+(^3P_0) + H_2(j=0)$, but the measured activation energy for the deuteriated analogue raises anew the question as to whether the energy represents a barrier or endoergicity. Other examples include the formation of weakly bound products such as HeN^+ and isotopic scrambling in $D_3^+ + H_2$ collisions. Finally, very recently measured ternary and radiative association rate coefficients $C_2H_2^+ + H_2 \rightarrow C_2H_4^+$ at 15 K are reported with special emphasis on the role of *ortho*- and *para*- H_2 . The perspectives are briefly discussed.

During the last years remarkable progress has been achieved in the development of experimental methods which allow one to study ion–molecule reactions under extreme conditions. A short overview of the different experimental methods which have been developed by several groups for the study of collisions at temperatures below 80 K, or at energies below 10 meV, will be given in the experimental section. A detailed and thorough discussion of low-temperature experiments can be found in a very recent article by Smith.¹

One of the major motivations for the experimental efforts is that low-temperature and low-density rate coefficients are needed for predicting the chemical evolution of interstellar clouds. Processes of specific interest include exothermic reactions which are hindered by a small barrier (*e.g.* $NH_3^+ + H_2 \rightarrow NH_4^+ + H$) or processes which are almost thermoneutral (*e.g.* $C_2H_2^+ + H_2 \rightarrow C_2H_3^+ + H$). Isotope-exchange reactions, belonging to the last class, are slightly endothermic in one direction due to differences in zero-point energies (*e.g.* $^{13}C^+ + ^{12}CO$; -3.5 meV); this leads to the astrophysically important process of isotopic fractionation. A process of specific astrophysical importance is association *via* spontaneous emission of a photon, but many theoretical approaches face only a few experiments.

Although astrophysical applications have probably been the major stimulant for experimental studies of ion–molecule reactions at extremely low energies, these processes are very important from a fundamental point of view and it is an interesting question in collision dynamics as to what can occur if the total energy goes to zero or varies by only a few meV near this limit. One consequence is, especially with hydrogen targets, that only a small number of partial waves contribute to the formation of the collision complex. This simplifies quantum-mechanical calculations and one can expect experimentally observable dynamical effects such as resonances. Other effects that occur in very slow collisions

may be due to the fact that excitation of rotational or fine-structure states is the dominant contribution to the total energy. One theoretically well studied phenomenon (*see, e.g.*, ref. 2) is due to angle-dependent long-range electrostatic forces. Weak potential anisotropies cause orientation effects and lead to interesting capture dynamics, especially as a function of rotational states. Finally, low total energies lead to long collision complex lifetimes and rare processes such as radiative association or rearrangement *via* internal tunnelling can become chemically important. These long lifetimes are also often responsible for the fact that statistical models are very successful in predicting mass and energy flow in the complexes. In some cases there are interesting deviations due to dynamical restrictions, symmetry ‘selection’ rules, or non-adiabatic mixing.

A fundamental understanding of all these dynamical and non-statistical effects helps finally to improve the descriptions of the chemical evolution in interstellar space. This is also necessary since, meanwhile, refined observation methods have resulted in very detailed astrophysical information and the models of interstellar clouds have reached a state of sophistication, such that for certain key reactions more information than simply reliable low-temperature rate coefficients are needed. In many interstellar environments non-thermal conditions prevail and information on elastic, inelastic and state-specific reactive cross-sections are needed at energies from meV and eV. Also, the internal and translational energies of reaction products should be known in order to describe the competition between sequential processes such as relaxation and reactions better. One of the most prominent examples for non-equilibrium conditions is the often discussed interstellar *o*- H_2 /*p*- H_2 ratio. Owing to the rather weak coupling (most probably *via* $H^+ + H_2$ collisions³) the population depends on the age or history of the interstellar clouds. Another example concerns non-thermal effects in the synthesis of

ammonia in interstellar space, the importance of which has been discussed recently.⁴ Formation of NH_4^+ in sequential reaction steps will be used for illustration in the following.

This contribution summarizes recent experimental progress in low-energy and state-specific ion-molecule reaction dynamics, made with the rapidly developing method of guided ion beams, merged beams and variable-temperature radiofrequency (rf) ion traps. It is organized as follows. The brief description of the rf ion optics based experiments is integrated into a short overview of different low-temperature experimental methods. As new results, low-temperature rate coefficients and state-specific cross-sections are presented for several reaction systems. Some general remarks concerning future experiments using the versatility of the ion trap and the merged beam machine will conclude this paper.

Experimental

The most common method used to obtain low-temperature conditions is based upon cryogenic cooling using liquid N_2 . At and above 80 K a large body of kinetic and thermodynamic data of ion-molecule reactions has been obtained using the flowing afterglow technique first developed by Ferguson and co-workers⁵ and its refined versions, the variable-temperature selected ion flow tube (VT-SIFT) and the drift field technique (SIFDT) pioneered by Smith and Adams.^{6,7} There are only few results from the first versions of liquid-nitrogen-cooled rf ion traps.⁸⁻¹⁰ Temperatures below 80 K have been attained by cooling the walls of the interaction region with liquid helium. The first results from a low-temperature drift tube have been reported by Böhringer and Arnold,¹¹ while the first direct measurement of a radiative association process was performed by Barlow *et al.*^{12,13} using a liquid-helium-cooled Penning trap apparatus. The variable-temperature rf ion trap which will be described below uses a closed-cycle refrigerator.

Experimental limitations in all these approaches are due to low vapour pressure and condensation and restrict the very low temperature studies to He or H_2 . This problem can be overcome by cooling the reactants in a supersonic expansion. One example is the CRESUS apparatus (cinétique de réactions en écoulement supersonique uniforme avec sélection) developed by Rowe *et al.*¹⁴ where ions of a selected mass are injected into the core of a supersonic flow of He which is several cm thick and up to 30 cm long and contains a small amount of the neutral molecules of interest. An extension to uniquely low temperatures has been made possible by the development of Smith and Hawley, who reached interaction temperatures between 0.1 and 20 K in a free jet flow reactor.^{1,15} In this experiment, a freely expanding mixture of gases is formed by expansion through a small nozzle orifice. Selective ionization is achieved by photoionization and analysis by a time-of-flight mass spectrometer. Complications are due to density gradients and temperature disequilibrium and the interpretation of the measured data requires a careful analysis of the cooling process, especially in mixed expansions.

A third approach to reaching very small relative energies is based on the well known merged beam method where kinematic compression allows one to reach meV collision energies. Early realizations^{16,17} used two very fast (keV laboratory energies) parallel beams. However, a variety of disadvantages (excited neutrals, low densities, short interaction time) and experimental problems (angular spread, overlapping volume) have impeded widespread use of this technique. The renaissance of the merged beam idea became possible by the guided ion beam method. Since the guiding fields allow one to operate with ion beams at laboratory energies below 100 meV, the fast neutral beam could be

replaced by a supersonic nozzle beam. This new method, which will be described below, has many advantages concerning high target density, cold neutrals and long interaction times. It is presently the only beam experiment with which state-specific cross-sections can be studied at meV collision energies.

Important criteria for characterizing all the mentioned experimental methods for astrophysical applications are the accessible density range, the sensitivity, and the versatility and reliability of the instrument. All swarm methods and supersonic flow reactors operate at rather high gas densities (reactant or buffer gas), which has the advantage of many thermalizing collisions but which often leads to higher-order reaction kinetics. For example high density impedes the study of radiative association processes due to ternary processes. Another limitation of the flow or swarm techniques is that the interaction time is determined by flight or drift times which are typically shorter than 1 ms. This sets an experimental limit on the minimum reaction rate coefficient which can be measured. It is a distinct advantage of ion-storage devices that the duration of the interaction time can be freely chosen since ions can be trapped without any loss for periods between microseconds and hours. With a suitable pumping capacity, the density of the target gas can be varied over many decades ($<10^9\text{--}10^{15}\text{ cm}^{-3}$), leading to a wide dynamic range. Extremely fast or very slow processes can be measured by optimizing the product of rate coefficient, density and interaction time. Especially important for astrophysical applications is that information on very slow processes such as radiative relaxation or radiative association can be derived.

The experimental results presented in this contribution have been obtained with two different machines, an ion trap and a merged beam apparatus. Both experiments make use of radiofrequency (rf) ion devices. The fundamental principle of particle confinement with fast oscillating forces and the characteristic features of such rf-field devices (ion sources, guides and traps for charged particles, energy and mass filters) have recently been discussed in detail.¹⁸ At sufficiently high frequencies the guiding and storage force can be derived from a so-called effective potential

$$V^* = q^2 E_0^2 / 4m\Omega^2 \quad (1)$$

which depends on the square of the charge q , on the local field strength E_0 , on the mass m and rf frequency Ω . It is always possible to choose operating conditions which can be characterized by an adiabaticity parameter, so that the total energy is an adiabatic constant of the motion. A variety of electrode arrangements have already been tested experimentally, the most prominent examples being the multipoles.

The ion trap used in the studies of this paper is depicted in Fig. 1. The 22-pole geometry leads to an effective potential proportional to r^{20} . The arrangement is mechanically more complicated than the recently described ring electrode traps;^{10,19} however, it has several advantages due to the axial geometry and the correction electrodes. The integration of the ion trap device into an ion beam apparatus and the individual elements of this apparatus (radiofrequency storage ion source, quadrupole ion guides *etc.*) have been described in detail elsewhere.¹⁸⁻²⁰ Reaction rate coefficients are determined from the temporal change of the ion composition which is measured by filling periodically the trap and extracting its content after various times. The target gas density is determined with a Leybold VISCOVAC VM 210 vacuum gauge; the collision temperature is derived from the temperatures of the trap electrodes and the walls of the surrounding environment, which are measured with adequate sensors (carbon resistor and gas thermometer).

A description of the first version of the merged beam

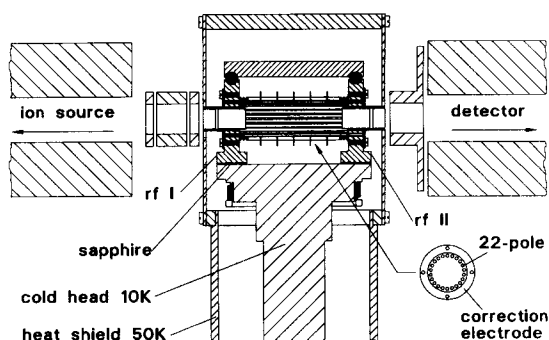


Fig. 1 The 22-pole ion trap is constructed from 22 1 mm rods equally spaced on an inscribed radius $r_0 = 5$ mm. The trap is mounted onto the cold head of a liquid-helium refrigerator using 0.5 mm thick sheets of sapphire to provide electrical insulation and very good thermal contact simultaneously. The trap is surrounded by a heat shield which is connected to the first stage (40–70 K) of the cryocooler. All connections to the trap, including the gas inlets and the wires to the rf coil are precooled to this temperature. A set of five thin electrodes can be used to correct the potential (with sub-mV accuracy) and to create suitable potential wells in the axial direction for different purposes. The entrance and exit electrodes are operated in a pulsed mode for ion injection and extraction, respectively. A quadrupole mass spectrometer is used to analyse the trap contents.

apparatus and details concerning the kinematics, the energy resolution and the lowest accessible energy, have been reported elsewhere.^{18,21} Meanwhile the apparatus has undergone two major modifications,^{22,23} which allows one to control both the internal temperature of the neutrals and of the primary ions between 10 and 300 K. The apparatus is shown schematically in Fig. 2. In both the ion trap and the merged beam machine the primary ions are created by electron bombardment, prethermalized in the high-pressure ion-storage source, selected according to mass and energy, and

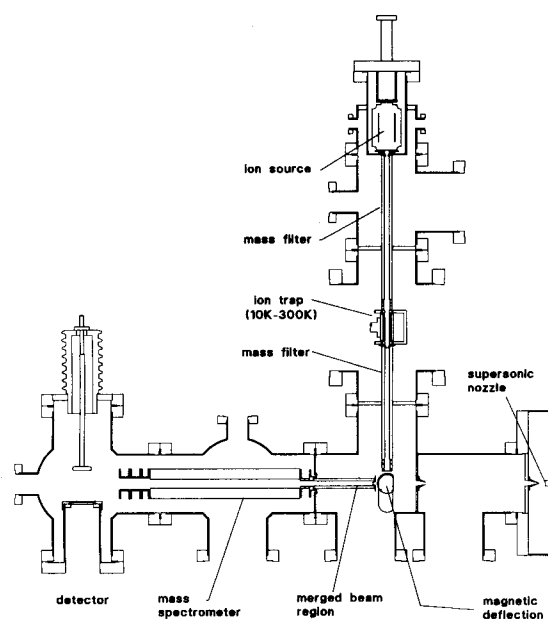


Fig. 2 Schematic diagram of the merged beam apparatus. The well collimated supersonic nozzle beam enters the merged beam region from the right *via* two differential pumping stages. Primary ions are prepared in a storage-ion source, mass selected and thermalized in a variable-temperature ion trap. After a second mass filter, the ions are merged into the neutral beam by deflection with a weak magnetic field (transmission energy < 1 eV). The interaction takes place in the merged beam region where the slow ion beam is guided in the weak field of an rf-only quadrupole. Primary and product ions are detected *via* a quadrupole mass spectrometer.

injected into a variable-temperature ion trap. Upon entering the ion trap, the ions undergo many collisions with the buffer gas, usually He, thereby adapting to the temperature of the trap environment. After a given trapping time, the ions are extracted from the trap.

In the ion trap machine the ions are mass-analysed and detected, while in the merged beam apparatus they enter a second mass filter, are deviated 90° in a weak magnetic field of < 1 kG and then injected at the desired energy into a weak rf guiding field. There they run coaxially with the neutral beam and can react at low relative energies. The temperature of the continuous supersonic beam can be varied by operating the nozzle either at 80 or 300 K and by using different expansion conditions.

Calibration of the ion axial energy is performed using time-of-flight methods. Both primary and product ions are guided to the quadrupole mass filter and detected with a standard scintillation detector. The directed centre-of-mass motion helps to reduce discriminating effects. To determine precisely the energy dependence of absolute integral cross-section a variety of tests are performed routinely (control of the spatial overlap of the two merged beams and determination of the velocity distributions of both beams using time of flight). In order to avoid confusion it must be noted that (for weak attenuation of the primary beam) the effective cross-section is calculated from

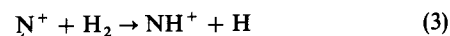
$$\sigma_{\text{eff}} = \dot{N}_p / \dot{N}_1 \frac{\langle v_1 \rangle}{\langle g \rangle} \frac{1}{\langle n_2 \rangle L} \quad (2)$$

where \dot{N}_1 is the primary, \dot{N}_p the product ion intensity, $\langle v_1 \rangle$ the mean velocity of the ions and $\langle g \rangle$ the mean relative velocity. All four values are measured quantities. The product $\langle n_2 \rangle L$, where L is the length of the overlapping volume and $\langle n_2 \rangle$ is the average density, is determined experimentally using reactions with known integral cross-sections such as $\text{Ar}^+ + \text{H}_2$. In some cases it is useful to present the data as effective rate coefficients, defined as $\langle g \rangle \sigma_{\text{eff}}$.

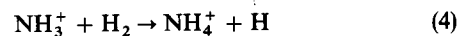
Results

The Ammonia Problem

One of the tentative explanations for the observed abundance of ammonia in dense interstellar clouds is based on a chain of H-atom abstraction reactions,^{4,24} starting with N^+ and the ion-molecule reaction



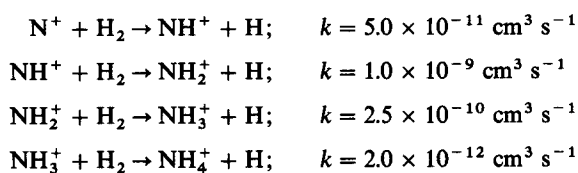
and ending with



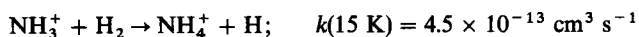
Dissociative electron ion recombination of NH_4^+ leads finally to NH_3 . Owing to their astrophysical relevance, reactions (3) and (4) have been the subject of intense experimental and theoretical investigations (see ref. 4, 25 and references therein). Both rate coefficients show strong temperature dependences, reaction (3) due to a slight endothermicity (details see below), while reaction (4) is certainly exothermic but hindered by a barrier and, therefore, can occur only *via* tunnelling at low energies.

To illustrate the features of the rf ion trap, the time evolution of this reaction sequence is shown in Fig. 3 (measured at 15 K and for two rather different $n\text{-H}_2$ densities). The lines are solutions of a simple master equation approach which accounts only for the elementary steps of H-abstraction. In

addition, the oversimplified assumption has been made that the rate coefficients



are independent of storage time, *i.e.* relaxation processes are ignored. It can be seen from the deviations between the lines and the data that these processes play a certain role. This is especially obvious in the case of NH_4^+ formation which is rather fast in the low-density measurement (upper panel) but the rate levels off as soon as all NH_3^+ ions formed are thermalized, as can be seen from the lower panel. A reliable thermal rate coefficient can be determined at high densities and long storage times (dashed line), resulting in



This value is in good agreement with theoretical and experimental results summarized in ref. 25.

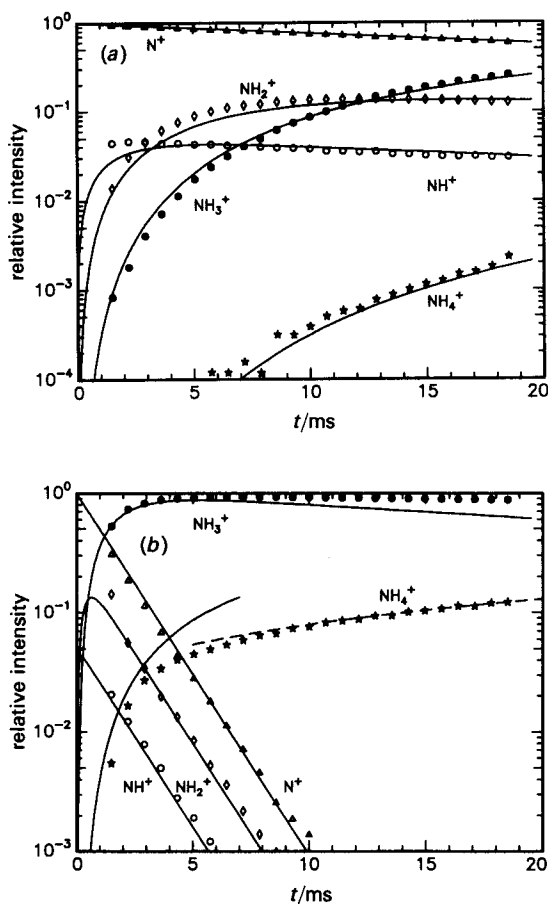


Fig. 3 Time evolution of the N^+ -based synthesis of ammonia studied in the 22-pole ion trap. The measurements were performed at 15 K and for two rather different $n\text{-H}_2$ densities (a) $5.6 \times 10^{11} \text{ cm}^{-3}$, (b) $1.4 \times 10^{13} \text{ cm}^{-3}$. The lines, which are in reasonable accord with the data, are solutions of a simplified rate equation approach. The deviations are partly due to thermalization of N^+ during the injection period (see NH^+ formation), and also due to the fact that the intermediate products are formed with internal and translational excitation. This is especially obvious in the case of NH_4^+ formation where thermal conditions are reached only at high densities and long storage times. The 15 K thermal rate coefficient is derived from a linear fit at late times [(b) dashed line].

$\text{N}^+ + \text{H}_2$ Reaction

The situation is less clear for reaction (3) in the context of formation of interstellar ammonia, as recently discussed by Galloway and Herbst.⁴ It has been concluded from a variety of experiments²⁶⁻²⁹ that formation of NH^+ requires a small activation energy. The large variation of the reported values (11–33 meV) is due to different experimental uncertainties but also due to difficulties in the interpretation of the results obtained with various methods. Since the activation energy is comparable with the rotational energy of the H_2 ($j = 1$, 14.4 meV) and also with the fine structure of N^+ ($^3\text{P}_1$, 6.1 meV; $^3\text{P}_2$, 16.2 meV), assumptions about the role of these different energy forms in driving the reaction have to be made if one measures averaged quantities.

The most conclusive experimental results are from the supersonic flow apparatus of Marquette *et al.*²⁹ Using both $n\text{-H}_2$ and $p\text{-H}_2$ it has been concluded that rotational energy is as efficient as translational energy in driving the reaction and an endothermicity of $\Delta H = 18 \pm 2$ meV has been deduced. The most consistent method which is presently available to estimate reaction endothermicities from averaged measured values is based upon phase-space calculations.³⁰ In order to evaluate the CRESU data, a dynamically biased statistical theory³¹ has been applied which has also taken into account the quadrupole moment of the H_2 and effects due to nuclear spin statistics. Treating the endothermicity as a free parameter, it has been concluded from the CRESU results that NH^+ formation requires 17 meV if both reactants are in their ground state. It is important to note that it was assumed in these calculations that spin-orbit energy is as efficient as translational energy.

New experimental studies of reaction (3) have been performed in the variable-temperature 22-pole trap. In these measurements rate coefficients are determined from the time-dependent attenuation of the N^+ ions. The two examples shown in Fig. 4 have been recorded at 15 K with $n\text{-H}_2$ and $p\text{-H}_2$. It is interesting that in both cases the N^+ intensity decreases with a single time constant over a wide range. It is almost certain that the N^+ ions, created externally by electron bombardment in the 350 K ion-storage source, are originally distributed statistically among the fine-structure states, *i.e.* $^3\text{P}_2 : ^3\text{P}_1 : ^3\text{P}_0 = 5 : 3 : 1$. Since, according to the assumptions of the phase-space calculations, the excited ions react faster, one would expect two breaks in the slope of the decay curve. The linear decay can be taken as an indication that the

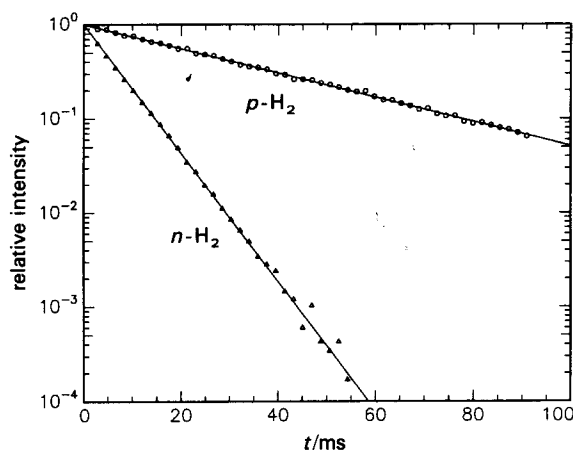


Fig. 4 Time-dependent attenuation of N^+ ions due to the endothermic bimolecular reaction $\text{N}^+ + \text{H}_2(j = 0, 1) \rightarrow \text{NH}^+ + \text{H}$ for normal hydrogen (Δ , $n\text{-H}_2$ density $3 \times 10^{12} \text{ cm}^{-3}$) and for >99% pure *para*-hydrogen (\circ , density $5 \times 10^{13} \text{ cm}^{-3}$) determined in the 22-pole ion trap at 15 K.

states relax very fast (in the first few ms) to the thermal 15 K equilibrium, *i.e.* almost exclusively to the 3P_0 ground state. However, it also cannot be excluded that the excited fine structure states do not react according to their additional energy.

In order to measure the temperature dependence of the rate coefficients, the N^+ intensity has been determined alternating between two storage times (typically between 10 and 20 ms). Densities between 10^{12} and 10^{13} cm^{-3} have been used. This allows one to obtain many discrete rate coefficients during the cooling phase of the cold head which typically takes 1 h. Results are shown as an Arrhenius plot in Fig. 5. For $n\text{-H}_2$ the figure contains three independent sets of data taken at different delay times. Fitting the data above 40 K leads to (units: $\text{cm}^3 \text{s}^{-1}$ and K)

$$k(100 > T > 40) = 2 \times 10^{-10} \exp(-41/T)$$

while the low-temperature behaviour is best described by

$$k(40 > T) = 1.1 \times 10^{-10} \exp(-26/T)$$

For $p\text{-H}_2$ a much steeper decline is observed which, however, levels off below 40 K. The two-exponential fit

$$k(T) = 1.4 \times 10^{-9} \exp(-230/T) + 5.4 \times 10^{-11} \exp(-24/T)$$

(dashed line) reveals that the slope at low temperatures is almost the same as that for $n\text{-H}_2$, a clear indication that the $p\text{-H}_2$ used contained some $o\text{-H}_2$ (3%). In another run, the admixture of $o\text{-H}_2$ was increased to 13% [circles, fit $k(T) \approx \exp(-29/T)$]. The lowest rate coefficients, which were measured with $p\text{-H}_2$ at 15 K ($k = 5 \times 10^{-13}$ $\text{cm}^3 \text{s}^{-1}$, diamonds), can be taken as an indication that the $o\text{-H}_2$ impurity level is <1%; however, other explanations such as traces of warm H_2 or HD impurities cannot yet be excluded.

The measured data are in good accordance with the CRESU results²⁹ and former rf ion-trap measurements.³¹ They are also in satisfactory agreement with the phase-space predictions (heavy lines) which have been calculated with the same parameters as given in ref. 31 ($\Delta H = 17$ meV, $f_r = 0.5$, $f_p = 1$, frozen nuclear spin). There are some minor deviations in the absolute values, which, at the present state of the experiment, may be due to uncertainties in the calibration of the temperature scale ($\pm 20\%$ or ± 5 K, whichever is larger).

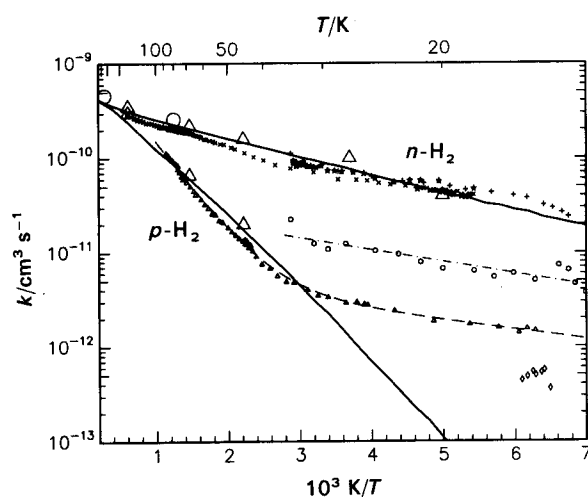


Fig. 5 Arrhenius plot of the thermal rate coefficient for the reaction $N^+H_2 \rightarrow NH^+ + H$ for $n\text{-H}_2$ (+, ×, ★, three different data sets) and for $p\text{-H}_2$ with different $o\text{-H}_2$ admixtures (○, 13%; △, 3%; ◇, <1%). The large triangles are CRESU results,²⁹ while the large circles are ring electrode trap measurements.³¹ The solid lines are phase-space calculations for $n\text{-H}_2$ and pure $p\text{-H}_2$. The two-exponential fit (dashed line) to the $p\text{-H}_2$ data is discussed in the text.

Also the difference in the slope of the $p\text{-H}_2$ data between 100 and 50 K is most probably due to this uncertainty. Nonetheless, it could also be imagined that the reactivity of the 3P_1 state, which is dominant in this temperature range, is not correctly described by the assumptions made in the phase-space theory.

In order to study separately the influence of translational, rotational and fine-structure energy in reaction (3), an experimental programme has been started using the merged beam apparatus depicted in Fig. 2. As a first result, Fig. 6 shows the energy dependence of the cross-section for reaction (3) for cold reactants plotted as effective rate coefficients $\langle g \rangle \sigma_{\text{eff}}$. In these measurements an effort has been made to approximate the ideal case $N^+(^3P_0) + H_2(j=0)$ by initially relaxing the ions in the trap using a 20 K He buffer and by expanding $p\text{-H}_2$ from a liquid-nitrogen cooled nozzle. For comparison, the figure contains the phase-space result for ground-state reactants. The decline of the rate coefficient with the collision energy and the fact that it falls below the 17 meV threshold is in qualitative accordance with theory; however, a quantitative agreement with the experiment is obtained only if N^+ is assumed to have an 80 K fine-structure population (solid line). An equally good fit can be obtained with the less likely assumption that the hydrogen target is characterized by 110 K and 75% $p\text{-H}_2$. More experiments to resolve the detailed threshold behaviour are in progress.

$N^+ + D_2$ Reaction

Substituting one or both of the hydrogen atoms with deuterium in reaction (3) leads to significant shifts in the endoergicity due to differences in zero-point vibrational energies. The occurrence of these differences is at least qualitatively clear from several experiments²⁷⁻²⁹ and it has been concluded from the consistency of the ΔH values with those calculated from the zero-point energies of reactants and products that the observed activation energy is due to a genuine endothermicity. From this one must conclude that reaction with D_2 must be 28.5 meV more endothermic than with H_2 , taking the energy values given in Table III of ref. 28. Therefore, an endothermicity of 45.5 meV has been used

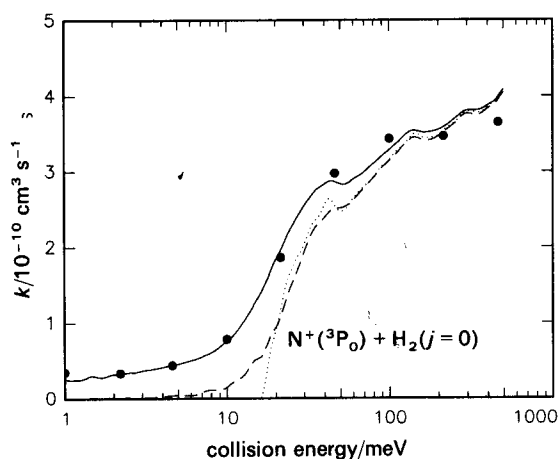


Fig. 6 Measured integral cross-sections (plotted as effective rate coefficients $k_{\text{eff}} = \sigma_{\text{eff}} \langle g \rangle$, where $\langle g \rangle$ is the mean relative velocity) for the reaction $N^+ + H_2 \rightarrow NH^+ + H$ for $p\text{-H}_2$ target and thermalized N^+ ions. The dotted line represents the phase-space theory for the ideal $N^+(^3P_0) + H_2(j=0)$ case, while consideration of the energy resolution of the merged beam apparatus leads to the dashed line. The heavy line is a phase space simulation (including experimental broadening), which is based on a 80 K thermal population of the N^+ fine-structure states.

in the phase-space calculations³¹ for predicting $N^+ + D_2$ rate coefficients. The results obtained are compiled in Table IIIc of ref. 31.

From the CRESU experiment²⁹ no endothermicity for reaction with D_2 was deduced since it was suspected that incomplete rotational relaxation in the flow resulted in an unknown amount of internal excitation. Thermal 350 and 80 K rate coefficients have also been measured in an rf ion trap³¹ where the problems with rotational relaxation can be excluded. The results were in good accordance with the CRESU results and already in ref. 31 the question was raised as to whether the endothermic behaviour is in reality caused by a barrier along the reaction path. New data for the temperature dependence of the ND^+ formation obtained with the variable-temperature 22-pole ion trap are shown in Fig. 7. The results are in full accord with former results (CRESU: triangles, ion trap: circles). As in Fig. 5 for $p-H_2$ the steep decline levels off below 50 K, indicating a small contribution from a less endothermic reaction. A two-exponential fit (units: $cm^3 s^{-1}$ and K) leads to

$$k(T) = 4.4 \times 10^{-10} \exp(-286/T) + 1.4 \times 10^{-12} \exp(-13/T)$$

In this case the second contribution can be fully accounted for by the small amount (*ca.* 0.3%) of HD impurities in the D_2 . Also the 45 K CRESU point is probably too large due to reactions with HD impurities. Preliminary 22-pole measurements with HD have resulted in low-temperature rate coefficients which have been fitted with

$$k(T) = 3.5 \times 10^{-10} \exp(-11/T)$$

in excellent agreement with the corresponding CRESU results.

In order to obtain agreement between experiment and theory, the phase-space calculations originally performed for $\Delta H = 45.5$ meV have been repeated at 35 meV and the results are shown as heavy line. As discussed above, the slight deviations in the slope of the new results can be due to uncertainties in the temperature scale. The derived activation energy of $\Delta H = 35$ meV is also consistent with experimental results from the merged beam apparatus described in the following.

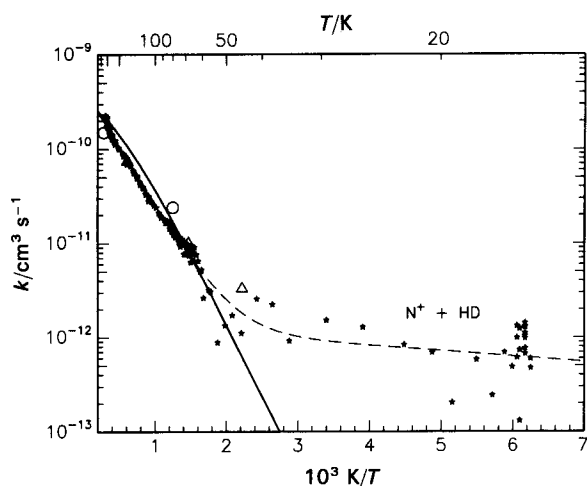


Fig. 7 Temperature dependence of the thermal rate coefficient for the reaction $N^+ + n-D_2 \rightarrow ND^+ + D$. The triangles and circles are CRESU²⁹ and ring electrode trap measurements,³¹ respectively. The heavy line is the result of a phase space calculation for $n-D_2$ with $\Delta H = 35$ meV. The dashed line is a two-exponential fit to the data (parameters see text). Comparison with $N^+ + HD$ measurements reveals that the low-temperature behaviour is due to HD impurities in the D_2 target gas (0.35%).

Fig. 8 shows integral cross-sections for reaction of N^+ ions with fully deuteriated target as a function of collision energy for two different target temperatures. The upper data points (filled circles) have been measured with the nozzle of the supersonic beam at room temperature, the lower ones (open circles) at 80 K. These temperatures are assumed also to be the final rotational temperature of the reactants since, as already mentioned, rotational cooling is very slow in hydrogen expansions and can be neglected under the conditions of the present experiment (nozzle diameter 0.1 mm, stagnation pressure 300 mbar). The measurements for a 300 K target have been performed with N^+ ions that possess a statistical population of the fine-structure states while in the 80 K D_2 measurements the N^+ ions have been stored for *ca.* 20 collisions in 20 K cold helium buffer gas; however, the efficiency of the relaxation is unclear.

These experimental data can be compared with properly weighted sums of state-specific phase-space cross-sections, $\sigma(E; I, j)$. Using thermal rotational populations at 300 and 80 K for D_2 , and assuming a 300 K thermal population of the three N^+ fine-structure states (in both cases), predictions for the two nozzle temperatures have been obtained (dotted lines). As reference, the figure also contains the phase-space cross-section for reaction of pure ground states with the onset at 35 meV. From the theoretical cross-sections the experimental observable functions (heavy lines) are calculated, accounting for the overall kinetic energy resolution of the apparatus. For the following discussion it is important to emphasize that both have been obtained in absolute units, *i.e.* there are no adjustable parameters.

The good agreement between phase-space and measured cross-sections at collision energies below 10 meV can be taken as an indication that the theory predicts quite accurately the dependence on the target temperature, *i.e.* the contribution of rotationally excited D_2 molecules and corroborates the ion trap result that the threshold for the reaction is 35 meV. Nonetheless there remain some inconsistencies concerning the role of the fine-structure energy, which may be due to incomplete relaxation of N^+ in He. Also, at energies above 10 meV, the calculated cross-section rises steeper than the measured one. This discrepancy cannot be removed by assuming a slightly higher threshold since this would reduce significantly the cross-section at low collision

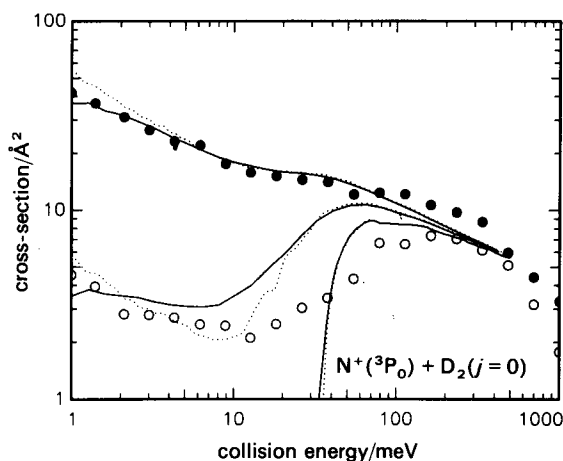


Fig. 8 Absolute integral cross-sections for the reaction $N^+ + D_2 \rightarrow ND^+ + D$ measured in the merged beam apparatus with two nozzle temperatures (\bullet , 300 K; \circ , 80 K). The dotted lines are properly weighted sums of state-specific phase space cross-sections (see text). Accounting for the experimental resolution leads to effective cross-sections, shown as solid lines. As a reference, the curves with the 35 meV threshold show the calculated cross-section for ground-state reactants.

energies and the thermal rate coefficients. It is important to note that the 80 K merged beam results are in excellent agreement with cross-sections determined recently in an independent experiment between 20 and 500 meV by Tosi *et al.*³² In this apparatus high energy resolution is achieved by crossing at 90° a low-energy guided ion beam with a supersonic molecular beam.

Despite the theoretical and experimental efforts to illuminate the behaviour of reaction (3) and its isotopic analogue in the threshold region, there remain several uncertainties, questions and wishes.

1. The best values for the endothermicities of the $N^+ + H_2$ and the $N^+ + D_2$ reaction are 17 and 35 meV, respectively. From this it must be concluded that the reactions are not hindered initially by a genuine endothermicity but by a barrier. Concerning the energetics, it would be desirable to establish the endothermicity from a spectroscopic characterization of NH^+ . The position and height of a potential barrier should be obtained from *ab initio* potential surfaces; some hints to a small saddle point due to an avoided crossing have been mentioned.³³

2. In the present measurements there are some inconsistencies concerning the role of the fine-structure energy. A quantitative evaluation of measurements performed for different N^+ temperatures requires more detailed tests of the relaxation process of the N^+ ions in the variable-temperature ion trap. These studies, using the merged beam apparatus as a state-specific detector, are interesting in themselves. For a detailed theoretical understanding of the role of the $N^+(^3P)$ fine-structure energy the coupling between the nine closely spaced spin-orbit ground-state surfaces has to be taken into consideration.

3. Apparently the phase-space theory can be used to reproduce the temperature dependence of the thermal rate coefficients and can describe those beam cross-sections where the total internal energy is already sufficient to drive the reaction. However, it seems to fail in predicting the detailed energy dependence of the cross-section in the vicinity of the threshold. This may be due to the influence of the first excited $NH^+ \ ^4\Sigma^-$ product state which lies less than 100 meV above the $^2\Pi$ ground state; however, it is by no means surprising if non-statistical reaction dynamics prevail, *e.g.* due to the barrier, the fine-structure coupling, or the interplay between the two strongly bound 3B_1 and 3A_2 surfaces of the NH_2^+ intermediate. More precise state-specific studies will contribute to the understanding of this elementary reaction. It also should be experimentally possible to obtain information on the rotational population of the NH^+ product states.

Formation of Weakly Bound Molecules

An important process that often occurs at low temperatures is the formation of weakly bound molecules *via* ternary or radiative association. For example, the growth of H_3^+ towards H_5^+ , H_7^+ and H_9^+ clusters has been followed at low temperatures in the ring electrode trap over 2 s at a H_2 density of $3.7 \times 10^{13} \text{ cm}^{-3} \text{ s}^{-1}$. The deduced rate coefficients for the sequential ternary association processes have been reported in ref. 19. Another example which is used here also to illustrate the sensitivity of the ion trap apparatus, is association of N^+ with He to HeN^+ . That N^+ can form a stable molecule with He was observed when attempts were made to study the $N^+ + H_2$ reaction in a SIFT experiment³⁴ at temperatures below 300 K; it was reported that the interaction of the N^+ ions with the helium carrier impeded the low-temperature determination of the NH^+ rate coefficient. Fig. 9 shows results from an experiment, performed in the 22-pole trap at a temperature of 15 K and an He density of

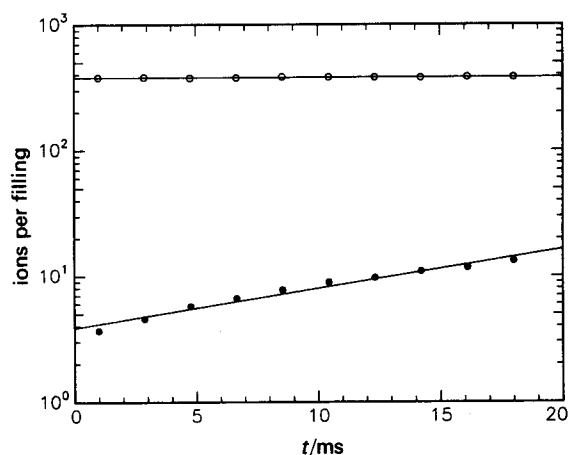


Fig. 9 Ternary formation of HeN^+ (●) molecules measured in the 22-pole trap at 15 K and at a density of $1.9 \times 10^{15} \text{ cm}^{-3}$. From an average of 380 N^+ ions (O) per filling *ca.* 12 ions are converted into HeN^+ after 20 ms storage time. The linear fit results in an apparent second-order rate coefficient of $8.7 \times 10^{-16} \text{ cm}^3 \text{ s}^{-1}$.

$4.8 \times 10^{14} \text{ cm}^{-3}$. The measurements have been performed at a repetition rate of 50 s^{-1} and, on average, 380 N^+ ions have been filled each time into the trap. After a storage time varying between 1 and 18 ms, the ion cloud was extracted and N^+ and HeN^+ were counted alternatively. The total accumulation time per data point was only 2 s, and the whole measurement took < 1 min. It is obvious that the attenuation of the N^+ ions is negligible while the number of products increases linearly (in 20 ms by 12.7 ions per filling). The fit results in an effective rate coefficient of $8.7 \times 10^{-16} \text{ cm}^3 \text{ s}^{-1}$ and a ternary rate coefficient of

$$k_3(15 \text{ K}) = 4.6 \times 10^{-31} \text{ cm}^6 \text{ s}^{-1}$$

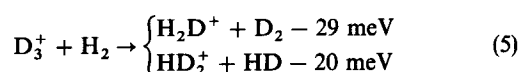
This value is so small that it would not lead to perturbations in a low-temperature SIFT experiment. Note, however, that the present value has been measured at 15 K, *i.e.* most probably with ground-state N^+ ions, and that the 3P_1 and 3P_2 states present in the SIFT above 80 K, may undergo much faster association with He.

Isotopic Fractionation

Reactions which involve solely the interchange of isotopes are close to being thermoneutral, but in most cases there is a slight endoergicity in one direction due to differences in zero-point energies. This endothermicity often explains why certain molecules are enriched in heavy isotopes at the low interstellar temperatures. From the point of view of collision dynamics, isotopic scrambling is a very interesting process which, in the case of identical particles, may be restricted due to exchange symmetries and where nuclear spin functions can play a significant role. Particularly large differences in binding energies occur in deuterium-proton substitution and more than 10 deuterated species have been identified in interstellar space.³⁵

The reaction of H_3^+ with H_2 has been studied quite often in various deuterated combinations. For example, the energy dependence of the integral cross-section for the exothermic proton transfer $H_3^+ + D_2 \rightarrow D_2H^+ + H_2$ has been measured at very low collision energies by means of the traditional merged beam technique³⁶ and also in the first version of the slow merged beam apparatus.^{18,21} Both sets of results show that the reaction occurs with a cross-section close to the Langevin limit. A VT-SIFT study of all possible deuterated $H_3^+ + H_2$ combinations has been published recently.³⁷

In order to study the competition between the two endothermic channels of the reaction



in the vicinity of the thresholds, integral cross-sections have been measured as a function of both translational and internal energy using the merged beam apparatus. The D_3^+ ions have been cooled in a 20 K cold buffer of $n\text{-D}_2$ gas before they enter the interaction region (see Fig. 2). The target beam was made from $n\text{-H}_2$, expanding from a 300 K nozzle. In qualitative accordance with the expectations, a significant decrease of the rate coefficients has been observed at low total energies,²² but a certain fraction of reactants has still maintained sufficient internal excitation to overcome the endoergicities of the two reactions. In order to observe more directly the threshold onset a pure $\text{H}_2(j=0)$ target beam and probably also colder D_3^+ ions have to be prepared.

The H_2D^+ channel in reaction (5) can be formed by a direct deuteron transfer mechanism while the production of the statistically favoured HD_2^+ ion requires a more complicated rearrangement process. These two distinct mechanisms can be used to explain the energy-dependent branching ratio $\sigma(\text{H}_2\text{D}^+) : \sigma(\text{HD}_2^+)$ shown in Fig. 10. The ratio above 1 indicates that already at rather low energies the collision time is so short that single deuteron transfer prevails. Only at collision energies below 20 meV, the statistically favoured HD_2^+ becomes dominant. The fact that the ratio reaches a limiting value of 1/2, which would be consistent with simple statistics, must be regarded as fortuitous since a correct statistical treatment has to account for the endoergicities, the symmetries, and for all three decay channels of the intermediate D_3H_2^+ complex.

For a quantitative analysis of the ratio one must also consider that in the present experiment the total energy of this complex is not only determined by the collision energy (resolution <10 meV), but also by the rotational energy of the hydrogen molecules in the beam (300 K expansion of

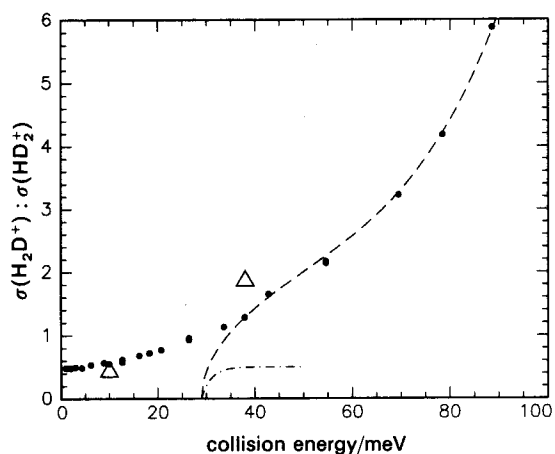


Fig. 10 Branching ratio $\sigma(\text{H}_2\text{D}^+) : \sigma(\text{HD}_2^+)$ for the two channels of the $\text{D}_3^+ + \text{H}_2$ reaction as a function of the collision energy measured with the merged beam apparatus with cold D_3^+ and an $n\text{-H}_2$ beam. The triangles are 80 and 300 K VT-SIFT³⁷ results, which have been plotted at $E_T = \frac{3}{2}k_B T$. With increasing energy, a direct reaction mechanism favours the single deuteron jump, producing H_2D^+ , while at low collision energies the statistically favoured H_2D^+ becomes dominant. If both reactants are in their ground state, the ratio should converge to zero at the threshold (29 meV) of the H_2D^+ . It is imaginable that the ratio retains the statistical value of 1/2 over a certain range (dash-dotted line) or that the direct deuteron transfer becomes dominant already at rather low energies (indicated by the dashed line).

$n\text{-H}_2$ in the depicted data) and by the internal energy of the D_3^+ primary ions (probably higher than 20 K). If both reactants are in their lowest states, the ratio $\sigma(\text{H}_2\text{D}^+) : \sigma(\text{HD}_2^+)$ must converge to zero at the threshold (29 meV) of the H_2D^+ channel. It is presently unclear whether, at total energies just above the threshold, the HD_2^+ product would remain favoured over a certain energy range as indicated by the dashed-dotted line or whether the ratio might increase as indicated by the dashed line.

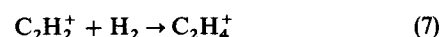
It is interesting to compare the merged beam results with the recently reported 300 and 80 K VT-SIFT ratios;³⁷ however, one has to be aware of the different experimental conditions. The 300 K value, plotted at a collision energy of $\frac{3}{2}k_B T$, is larger than the merged beam ratio at this collision energy. This is consistent with the fact that the reactants have a mean internal energy below 300 K. The opposite behaviour can be seen for the 80 K ratio, and one can conclude that a mean complex energy, corresponding to a temperature of 80 K, is reached in the beam experiment only at the lowest collision energy.

Radiative Association of $\text{C}_2\text{H}_2^+ \cdot \text{H}_2$

The importance of radiative association in interstellar chemistry has been recognized for more than 20 years; however, experimental studies have become routine only recently. The progress which became possible by the development of suitable ion-storage techniques has been reviewed very recently.²⁰ Under most experimental conditions the stabilization of a collision complex by emission of a photon competes with the stabilization by a third body. At low densities, the process can be described by the apparent second-order rate coefficient³⁸

$$k^* = k_3[\text{B}] + k_r \quad (6)$$

where k_3 is the termolecular rate coefficient, [B] the density of the third body B, and k_r the bimolecular rate coefficient for radiative stabilization. Experimental information on both stabilization processes has been obtained for the association reaction



by studying C_2H_4^+ formation at 80 K over a wide density range (10^{11} – $3 \times 10^{13} \text{ cm}^{-3}$) in the ring electrode ion trap and by measuring k_3 at temperatures between 35 and 150 K for $n\text{-H}_2$ and $p\text{-H}_2$.²⁰ A thorough discussion of these experimental results is given in Herbst's contribution to this Faraday symposium³⁸ and the majority of the experimental findings are nicely reproduced by his phase-space calculation (zero-barrier version). The only noticeable and presently unexplained discrepancy between experiment and theory is the ratio $k_3(n\text{-H}_2)/k_3(p\text{-H}_2)$ at temperatures >60 K.

Fig. 11 shows some new results obtained at the lowest temperature presently attainable in the 22-pole trap ($15 \pm 5 \text{ K}$). In order to determine both the radiative and the ternary rate coefficients, the density of the hydrogen has been varied over three orders of magnitude. The figure contains measurements both for $n\text{-H}_2$ and $p\text{-H}_2$. The dashed lines are best fits of eqn. (6) to the data, resulting in the following set of parameters

$$\begin{aligned} p\text{-H}_2(15 \text{ K}); & \quad k_3 = 1.6 \times 10^{-24} \text{ cm}^6 \text{ s}^{-1}; \\ & \quad k_r = 4.6 \times 10^{-12} \text{ cm}^3 \text{ s}^{-1} \\ n\text{-H}_2(15 \text{ K}); & \quad k_3 = 3.6 \times 10^{-25} \text{ cm}^6 \text{ s}^{-1}; \\ & \quad k_r = 1.3 \times 10^{-12} \text{ cm}^3 \text{ s}^{-1} \end{aligned}$$

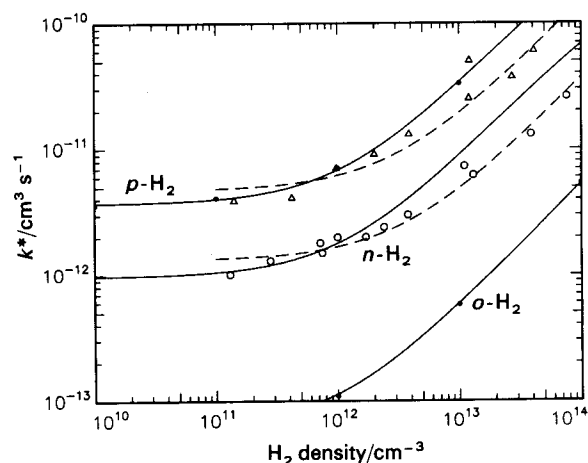


Fig. 11 Effective rate coefficients k^* for associative $C_2H_4^+$ formation as a function of H_2 gas density. Experimental results have been obtained for both *para* (triangles) and normal (open circles) hydrogen at a temperature of 15 ± 5 K. The dashed lines represent fits to $k^* = k_3[H_2] + k_r$. The small solid dots are Herbst's phase space calculation for *o*- H_2 and *p*- H_2 at 2 K (see Fig. 5 of ref. 38); the solid lines interpolating the phase space data, have been used to calculate the *n*- H_2 curve.

There are some indications for deviations from the simple functional form given by eqn. (6). At present, the quality of the data is not yet sufficient to use the three- or even six-parameter fit which would give, as described in ref. 20, hints to two-complex mechanism, complex lifetimes, stabilization efficiencies and saturation effects.

Fig. 11 also shows three functions (heavy lines) which fit for *p*- H_2 and *o*- H_2 the apparent second-order rate coefficients calculated at 2 K as a function of the density (solid dots).³⁸ The two outer curves are interpolations through the *p*- H_2 and *o*- H_2 data, while the middle curve is a 1:3 weighted sum of the two functions, *i.e.* the theoretical prediction for *n*- H_2 . It is surprising how good the statistical theory describes the *ortho/para* influence. By comparing theory and experiment in detail one has to consider that they refer to different temperatures; however, there is both experimental and theoretical evidence that, below 30 K, the rate coefficients k_3 and k_r are only weakly dependent on temperature ($\propto T^{-n}$ with $n < 1$). The ternary rate coefficients are in qualitative accordance with this trend, while it is somewhat surprising that the measured 15 K radiative association rate coefficient is almost identical with the calculated 2 K value.

Comparison of the present 15 K value $k_3(n-H_2) = 3.6 \times 10^{-25} \text{ cm}^6 \text{ s}^{-1}$ with the free-jet flow reactor results¹⁵ which are approximately described by $k_3(1.5 < T/K < 3) = 3.7 \times 10^{-24} T^{-3} \text{ cm}^6 \text{ s}^{-1}$ reveals several discrepancies. The difference in the absolute value [*i.e.* $k_3(3 \text{ K}) = 1 \times 10^{-25} \text{ cm}^6 \text{ s}^{-1}$] can partly be explained by saturation effects due to the rather high density in the free jet.³⁸ The steep temperature dependence, however, can only be a local change in reactivity if it is real. There are also still some unexplained inconsistencies with the bimolecular $C_2H_3^+$ channel which has been observed to be quite efficient at temperatures below 3 K.¹⁵ Recent 22-pole experiments indicated a value of $k < 10^{-13} \text{ cm}^3 \text{ s}^{-1}$ at 15 K; however, the precise determination of this rate coefficient is complicated by a large $C_2H_3^+$ background which is created from hot $C_2H_2^+$ ions before they are thermalized to the ambient trap temperature. More experiments, with H_2 and He as buffer gas and with deuteriated reactants, are in progress. From the point of view of astrophysical applications, the 22-pole results indicate that the formation of $C_2H_4^+$

via radiative association is more important than the bimolecular $C_2H_3^+$ production. This is also in accordance with the phase-space theory.³⁸

Conclusions

Remarkable experimental progress has been achieved in the last ten years in the field of low-temperature ion-molecule reactions. Part of the new experimental progress has become possible by the development of rf-based devices, the versatility of which has been illustrated in this contribution and recently through a larger variety of applications.¹⁸ The development of innovative techniques leads to new experimental insight but also often raises new questions, the $N^+ + H_2$ and the $C_2H_2^+ + H_2$ reactions being typical examples. More experimental and theoretical studies are needed to understand the detailed role of electronic and rotational energy or the influence of barriers and tunnelling on reactivity. The versatility and high sensitivity of the variable-temperature rf ion trap method has opened a wide field of experiments, also of astrophysical interest. Most important is that measurements of radiative association processes are now becoming routine and for several systems, reliable low-temperature results have been reported.²⁰ It is clear that the present versions of the merged beam and the ion-trap apparatus can be applied to numerous systems and many problems.

Looking to the future, a straightforward extension of the merged beam technique is the use of a seeded beam of polar molecules (*e.g.* NH_3 , H_2O seeded in He). Owing to the very large rate coefficients of ion-dipole reactions ($k > 10^{-8} \text{ cm}^3 \text{ s}^{-1}$), the effect of rotational motion could be studied at meV collision energies using different expansion conditions. It should also be possible to detect radiative association processes for systems such as $CH_3^+ + H_2O \rightarrow CH_3OH_2^+$ provided their rate coefficient are sufficiently large.³⁹ Other experimental developments and improvements are imaginable. For example, future extensions could make use of a supersonic beam of H, C, N or O atoms to study reactions which are important for dense-cloud chemistry such as $H_3^+ + C$.

There are also other applications of the ion trap besides measurements of temperature and density-dependent rate coefficients. Laser-based methods can be used to obtain spectroscopic information on cold stored ions, or to study state-specific reactions by modifying the low-temperature equilibrium *via* continuous laser pumping of an infrared transition of the stored ions. These kinds of experiments could also be extended to observe the competition between association and photofragmentation.

Since all of these experiments can be performed at temperatures or energies of astrophysical interest, it is expected that many of the results will help to model or increase our understanding of interstellar chemistry.

This work is the result of a common effort of several people. Dr G. Kaefer and Dipl. Phys. W. Paul constructed and tested the first variable-temperature rf ion traps. Much progress has been initiated by Dr S. Horning, who stayed for more than a year as an Alexander von Humboldt research fellow in our research group. Dipl. Phys. A. Sorgenfrei developed the 22-pole ion trap and performed the recent experiments. The first contributions to the merged beam apparatus are due to Dipl. Phys. H. Kalmbach, while the results presented in this contribution are due to Dipl. Phys. O. Wick. The author is especially indebted to Professor Ch. Schlier for his continuous interest and contributions to this work. Many thanks are also due to Professor M. Smith for stimulating dis-

cussions and helpful advice. Financial support of the Deutsche Forschungsgemeinschaft (SFB 276) is gratefully acknowledged.

References

- M. A. Smith, *Ion-Molecule Reaction Dynamics at Very Low Temperatures*, in *Current Topics in Ion Chemistry and Physics*, ed. C. Y. Ng, T. Baer and I. Powis, Wiley, New York, 1993, vol. 2.
- D. C. Clary, in *Rate Coefficients in Astrochemistry*, ed. T. J. Millar and D. A. Williams, Kluwer, Dordrecht, 1988.
- D. Gerlich, *J. Chem. Phys.*, 1990, **92**, 2377.
- E. T. Galloway and E. Herbst, *Astron. Astrophys.*, 1989, **211**, 413.
- E. E. Ferguson, in *Ion-Molecule Reactions*, ed. J. L. Franklin, Butterworths, London, 1972, vol. 2, ch. 8.
- D. Smith and N. G. Adams, *Mon. Not. Roy. Astron. Soc.*, 1981, **197**, 377.
- D. Smith and N. G. Adams, *Adv. At. Mol. Phys.*, 1988, **24**, 1.
- D. Gerlich, G. Kaefer, *Proc. 5th Int. Swarm Seminar*, ed. N. G. Adams and D. Smith, Birmingham University, 1987, p. 133.
- D. Gerlich and G. Kaefer, *Symp. on Atomic and Surface Physics*, ed. A. Pesnelle, F. Gounand, M. Cheret and F. Fabre, La Plagne, France, 1988, p. 115.
- D. Gerlich and G. Kaefer, *Astrophys. J.* 1989, **347**, 849.
- H. Böhlinger and F. Arnold, *Int. J. Mass Spectrom. Ion Phys.*, 1983, **49**, 61.
- S. E. Barlow, G. H. Dunn and M. Schauer, *Chem. Phys. Lett.*, 1984, **52**, 902.
- S. E. Barlow, G. H. Dunn and K. Schauer, *Chem. Phys. Lett.*, 1984, **53**, 1610.
- B. R. Rowe, J. B. Marquette and C. J. Rebrion, *J. Chem. Soc., Faraday Trans. 2*, 1989, **85**, 1631.
- M. Hawley and M. A. Smith, *J. Chem. Phys.*, 1992, **96**, 1121.
- S. M. Trujillo, R. H. Neynaber and E. W. Rothe, *Rev. Sci. Instrum.*, 1966, **37**, 1655.
- U. Giese and R. Gentry, *J. Chem. Phys.*, 1975, **62**, 1364.
- D. Gerlich, *Inhomogeneous Electrical Radio Frequency Fields: A Versatile Tool for the Study of Processes with Slow Ions*, in *State-selected and State-to-state Ion-Molecule Reaction Dynamics*, ed. C. Y. Ng and M. Baer, *Advances in Chemical Physics Series LXXXII*, Wiley, New York, 1992.
- D. Gerlich, G. Kaefer and W. Paul, in *Symp. on Atomic and Surface Physics*, ed. T. D. Märk and F. Howorka, Just, P. Jonenphysik, Innsbruck, 1990, p. 332.
- D. Gerlich and S. Horning, *Chem. Rev.*, 1992, **92**, 1509.
- D. Gerlich, in *XII Int. Symp. on Molecular Beams*, ed. V. Aquilanti, Perugia, 1989, p. 37.
- D. Gerlich, H. J. Jitschin and O. Wick, in *Symp. Atomic and Surface Physics*, ed. D. Bassi, M. Scotini and P. Tosi, Pamepego, 1992.
- O. Wick and D. Gerlich, unpublished results.
- E. Herbst and W. Klemperer, *Astrophys. J.*, 1973, **185**, 505.
- E. Herbst, D. J. DeFrees, D. Talbi, F. Pauzat, W. Koch and A. D. McLean, *J. Chem. Phys.*, 1991, **94**, 7842.
- J. Luine and G. Dunn, *Astrophys. J.*, 1985, **299**, L67.
- N. G. Adams and D. Smith, *Chem. Phys. Lett.*, 1985, **117**, 67.
- K. M. Ervin and P. B. Armentrout, *J. Chem. Phys.*, 1987, **86**, 2659.
- J. Marquette, C. Rebrion and B. Rowe, *J. Chem. Phys.*, 1988, **89**, 2041.
- J. C. Light, *J. Chem. Phys.*, 1964, **40**, 3221.
- D. Gerlich, *J. Chem. Phys.*, 1989, **90**, 3574.
- P. Tosi, O. Dmitrijev, D. Bassi, O. Wick and D. Gerlich, *Chem. Phys. Lett.*, to be submitted.
- U. Wilhelmsson, P. E. M. Siegbahn and R. Schinke, *J. Chem. Phys.*, 1992, **96**, 8202.
- D. Smith and N. G. Adams, in *Rate Coefficients in Astrochemistry*, ed. T. J. Millar and D. A. Williams, Kluwer, Dordrecht, 1988, p. 153.
- A. Wootten, in *Astrochemistry*, ed. M. S. Vardya and S. P. Tarafdar, Reidel, Dordrecht, 1987, p. 311.
- C. H. Douglass, G. Ringer and W. R. Gentry, *J. Chem. Phys.*, 1982, **76**, 2423.
- K. Giles, N. G. Adams and D. Smith, *J. Phys. Chem.*, 1992, in the press.
- E. Herbst and K. Yamashita, *J. Chem. Soc., Faraday Trans.*, 1993, **89**, 2175.
- D. R. Bates and E. Herbst, in *Rate Coefficients in Astrochemistry*, ed. T. J. Millar and D. A. Williams, Dordrecht, Kluwer, 1988, p. 17.

Paper 2/06063I; Received 12th November, 1992